Band structure and itinerant magnetism of iron-arsenide superconductors

L. Boeri and O.K. Andersen

The discovery of superconductivity with $T_c \leq 26$ K in F-doped LaOFeAs [1] has initiated an intense theoretical and experimental activity, leading to the discovery of the new, rich family of Fe-based superconductors (FeBSC). The low values of the electron-phonon coupling constants predicted by ab initio calculations [2], and the simultaneous presence of superconductivity and (antiferro)-magnetism in the phase diagram, suggest that superconductivity is most likely of electronic origin. Several features of FeBSC, such as their multiband nature, itinerant magnetism and moderate electronic correlations, complicate the understanding magnetism and superconductivity in these materials; even the results of standard Local Spin Density Approximation (LSDA) calculations are regarded as puzzling. Here, we explain in detail the LSDA band structure and magnetic response of LaOFeAs, as a prototype for Fe-based superconductors, in terms of a Stoner model for weak-coupling itinerant magnetism, based on an analytical Tight-Binding (TB) model.

The crystal structure of LaOFeAs, shown in Fig. 1(a), consists of alternating $(LaO)^+$ and $(FeAs)^-$ layers. The $(LaO)^+$ layers play essentially no role in superconductivity, but their presence is needed to stabilize the structure. The $(FeAs)^-$ layers are the common building block of all Fe-based superconductors. Figure 1(b) shows a top view: Fe atoms form a square lattice, at the center of $FeAs_4$ tetrahedra, formed by parallel chains of As atoms, sitting above/below the Fe planes (full/empty symbols in the figure). The critical temperature T_c of Fe pnictides correlates empirically with the distortion of the $(FeAs_4)$ tetrahedra, in such a way that T_c is highest when the tetrahedra are ideal. The three-dimensional unit cell of LaOFeAs, shown in Fig. 1(a), contains two formula units. The isolated FeAs layer possesses an additional translational-mirror symmetry operation, which permits to reduce to a single FeAs unit cell. The corresponding 2D Brillouin zone is shown in Fig. 1(c). For simplicity, we will use the 2D notation throughout the paper.

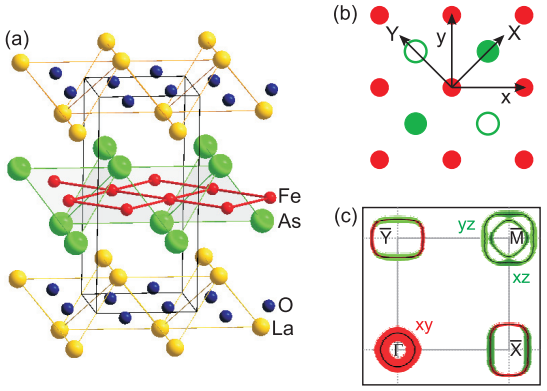

Figure 1: LaOFeAs: (a) Crystal structure; (b) Top view of an Fe–As plane; the reduced unit cell contains a single FeAs unit. The x and y axes are directed along Fe–Fe bonds, whereas the X and Y axes are directed along Fe–As bonds, respectively. (c) Two-dimensional Brillouin zone and Fermi surface, decorated with t_{2g} partial characters. Special $\mathbf{k}$ points: $\bar{\Gamma} = (0,0)$; $\bar{X} = (\pi,0)$; $\bar{Y} = (0,\pi)$; $\bar{M} = (\pi,\pi)$.

The ground state of undoped LaOFeAs is a stripe-type metallic antiferromagnet, in which the Fe spins are aligned ferromagnetically (FM) along one of the Fe–Fe bond, and antiferromagnetically (AFM) along the other Fe–Fe bond, respectively (Fig. 1(b)). The magnetic transition is accompanied by a tetragonal to orthorhombic distortion, which expands the bond length in the AFM direction (y) and contracts it in the FM one(x). The magnetic moment is small $m = 0.3\,\mu_B$. Doping with holes or electrons destroys the SDW order and induces superconductivity, with $T_c \leq 26$ K. The stripe AFM order corresponds to a SDW with $\mathbf{Q} = (0,\pi)$, which is a nesting vector connecting the hole and electron portions of the LDA non-magnetic Fermi surface, shown in Fig. 1(c).

Ab initio calculations give results which are apparently consistent with the experiment, but significant discrepancies exist. Calculations based

on the Local Spin Density Approximation (LSDA) correctly predict that the ground state of the undoped compound is a striped $\mathbf{Q} = (0,\pi)$ SDW metal, but yield a value of the magnetic moment ($m \approx 2\mu_B$ in the Generalized Gradient Approximation – GGA), which is too large compared to experiment. Consistently, the Fermi surfaces in the ordered phase are very different from those observed experimentally, which resemble much more the non-magnetic (NM) picture, shown in Fig. 1(c). On the other hand, the lattice properties related to the FeAs bonds can only be reproduced by spin-polarized LSDA calculations, suggesting that a large ($m \approx 2\mu_B$) magnetic moment is needed to obtain a good picture of the bonding [2]. At the same time, the value of the LSDA self-consistent magnetic moment is strongly sensitive to the change in FeAs bonds, and in particular to the distortion of the $FeAs_4$ tetrahedra.

In order to understand the origin of this unusual disagreement between first-principles calculations and experiment, in the following we discuss the formation of the AFM moment in LSD calculations. We show that the same, mean-field, itinerant model for magnetism, possesses both a small-moment ($m \approx 0.3\mu_B$) solution at weak coupling, and a large-moment ($m \approx 2\mu_B$) solution at intermediate coupling. While the first is strongly connected to Fermi surface nesting, and thus easily destroyed, the second involves a much larger region of the non-magnetic band structure, and is much more robust.

For this, we first derive an analytical TB Hamiltonian for the NM band structure of LaOFeAS derived *ab initio* downfolding the full band structure onto a basis formed by five Fe *d* and three As *p* orthonormalized orbitals. Then, we study a Stoner model for weak-coupling itinerant (anti)ferromagnetism.

In our TB model, we choose to include the As *p* orbitals explicitly into the basis, in order to study the effects of the strong As *p* - Fe *d* covalency, which is crucial in these materials. In fact, it would be possible to describe accurately all the features of the band structure of LaOFeAs in an energy window of ± 2 eV around E_F also using a smaller basis set, formed by the five Fe *d* orbitals shown in Fig. 2. However, the orbitals are very extended, and strongly deformed with respect to their atomic shape, due to a sizable hybridization with As *p*-states. The effect is larger for the three t_{2g} (*Xz*,*Yz*,*xy*), than for the two e_g (*XY* and *zz*) orbitals. In Fig. 3 we show that, when the As *p*-orbitals are included into the basis set, the Fe *d*-orbitals localize. What causes the long range of the orbitals (and hoppings) of the model shown in Fig. 2 is thus the hybridization with the diffuse As *p*-orbitals. Together, the two sets of pictures show that the bonding in LaOFeAs is characterized by a strong covalency between localized Fe *d*- and diffuse As *p*-states. The largest *p*–*d* matrix elements (X/Xz,Y/Yz, z/xy) are odd with respect to the Fe planes, and thus strongly sensitive to the tetrahedral angle.

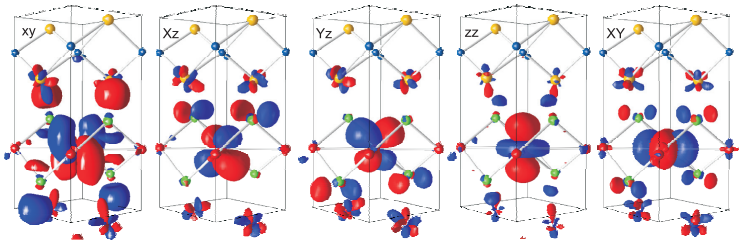

Figure 2: Wannier functions of LaOFeAS, obtained by downfolding the full band structure on a basis set formed by five Fe *d* NMTO's, which span the 5 energy bands at ± 2 eV around E_F in Fig. 4. Positive (negative) isocontours are shown in red(blue). For the definition of axes see Fig. 1(b). *XY* is short for $x^2 - y^2$, *zz* is short for $3z^2 - r^2$.

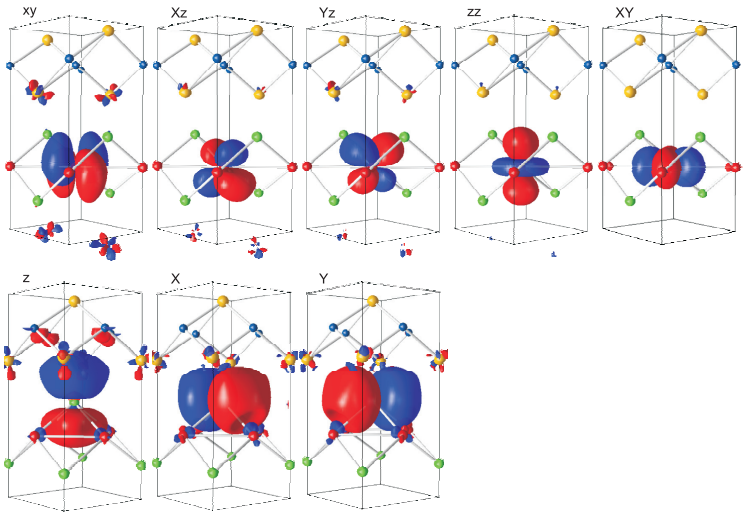

Figure 3: Same as Fig. 2, but for a basis set comprising five Fe d (top) and 3 As p (bottom) NMTO's, spanning all eight bands shown in Fig. 4.

Figure 4 shows the NM band structure of LaOFeAs, decorated with a 'fatness' proportional to the individual characters of the Fe d and As p Wannier orbitals shown in Fig. 3. With Fe in a d^6 configuration, there are twelve electrons to accommodate in the eight bands, which extend from –5 eV to 3 eV. There is a gap in the electronic spectrum at –2 eV, separating the three lowest bands, which mainly have As p-character, from the remaining five, which mainly have Fe d-character. The two e_g bands (zz and XY) hybridize with each other, and gap almost everywhere around the Fermi energy. The bands at the Fermi level are predominantly of t_{2g} character; the Fermi surface, shown in Fig. 1(c), consists of two degenerate, M centered *hole* pockets with xz,yz character, a singly-degenerate *hole* pocket centered at Γ, and two ellipsoidal *electron* pockets at X(Y), formed by xy/z and xz(yz)/y(x) bands, respectively.

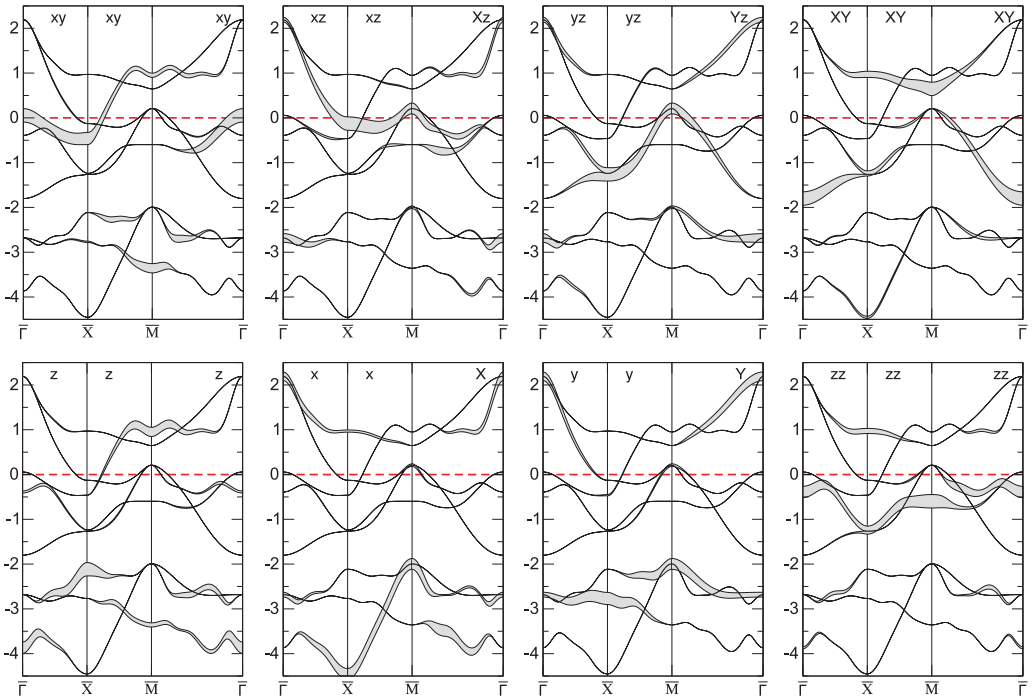

Figure 4: 'Fat' bands of p–d model; the fatness of the bands is proportional to the partial character associated to the orbitals shown in Fig. 3. Energies are measured with respect to the Fermi level. The corresponding Fermi surfaces are shown in Fig. 1(c).

In Fig. 4, the significant Fe–As hybridization seen in the orbitals shows up as shared *p–d* fatness; close to the Fermi level, it affects the dispersion of all bands, and in particular it causes the *upwards* dispersion of the *xz*(*yz*)/*y*(*x*) bands that form the electron pockets. Furthermore, the long range of the Fe-As and As-As hoppings causes the masses of all Fermi surface pockets to be almost free-electron like.

This non-trivial NM electronic structure, characterized by a multiband, strongly nested Fermi surface and strong, long-range *p–d* hybridization, complicates the description of magnetism and superconductivity at any level of approximation. Here, we study antiferromagnetism using a simple Stoner model, which, for a fixed value of the exchange coupling constant I, is a good approximation to the self-consistent LSDA calculations. Starting from the Tight-Binding Hamiltonian $\hat{H}_0(\mathbf{k})$, we construct the Hamiltonian $H_{\rm SDW}(\mathbf{k})$ of a SDW with wavevector $\mathbf{Q}$ as:

$$\hat{H}_{\rm SDW}(\mathbf{k}) = \begin{pmatrix} \hat{H}_0(\mathbf{k}) & \hat{\Delta}/2 \\ \hat{\Delta}/2 & \hat{H}_0(\mathbf{k}+\mathbf{Q}) \end{pmatrix}, \qquad (1)$$

where $\hat{\Delta}$ is a diagonal matrix, with $(\hat{\Delta})_{\rm Fe,Fe} = \Delta\hat{1}$ $(\hat{\Delta})_{\rm As,As} = \hat{0}$. This corresponds to applying a staggered magnetic field $\pm\Delta/2$, which induces a staggered magnetic moment $\pm m/2$ with the periodicity of the SDW. The spin-polarized band structure is then obtained diagonalizing the Hamiltonian (Eq. (1)); the magnetic moment is then given by: $m = \sum_{\rm i}\sum_{\mathbf{k}} c^{\star}_{{\rm i},\mathbf{k}} c_{{\rm i},\mathbf{k}+\mathbf{Q}}$, where $c_{{\rm i},\mathbf{k}+\mathbf{Q}}$ are the eigenvectors of the matrix (Eq. (1)). At equilibrium, a self-consistent condition relates m to Δ through the Stoner coupling constant I:

$$\Delta = m\, I \qquad (2)$$

In Fig. 5, we show the bare susceptibilities, $\chi_0(m) = m(\Delta)/\Delta$, as a function of the induced moment $m(\Delta)$, for striped $-\mathbf{Q} = (0,\pi)-$ (left) and checkerboard $-\mathbf{Q} = (\pi,\pi)-$ (right) AFM order, obtained by solving Eqs. (1) and (2) as a function of Δ. The electron-doping x, is modeled by a rigid shift of the Fermi level. On these plots, the self-consistency condition Eq. (2) is given by the intercept of the $\chi_0(m)$ curve with a line $m/\Delta = 1/I$.

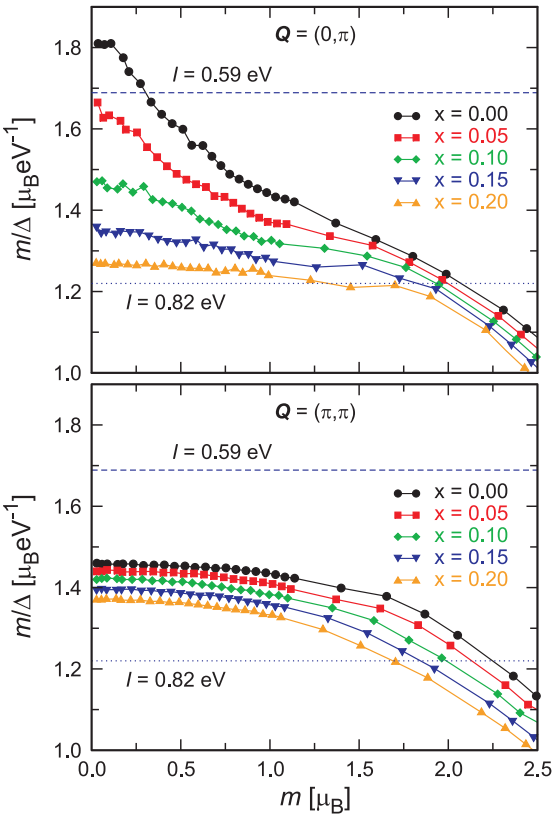

Figure 5: (a) Bare susceptibilities $\chi_0(m) = m(\Delta)/\Delta$ as a function of the induced magnetic moment m, for $LaO_{1-x}F_xFeAs$, for striped (Ȳ) and (b) checkerboard (M̄)(*b*) SDW order, Eqs. (1) – (2). The two horizontal lines on the plot mark the two values of I which correspond to the value of the magnetic moment observed experimentally ($m = 0.3$, $I = 0.59$ eV), and to that given by LSDA-GGA calculations ($m = 2.0$, $I = 0.82$ eV) for $x = 0$.

The two horizontal lines indicate the two values of I, which give the experimental value ($m = 0.3\,\mu_{\rm B}$, $I = 0.59$ eV), and the LSDA value ($m = 2.0\,\mu_{\rm B}$, $I = 0.82$ eV) for the magnetic moment at $x = 0$ and $\mathbf{Q} = (0,\pi)$. Within the itinerant Stoner model, a 20% reduction of I is thus sufficient to bring the value of the magnetic moment from the large LSDA value $m = 2.0\,\mu_{\rm B}$, to a value which is much closer to experiment $m \approx 0.3\,\mu_{\rm B}$. Furthermore, this small-moment solution is not found for the checkerboard order with $\mathbf{Q} = (\pi,\pi)$, and is rapidly suppressed by doping, in agreement with experiment. The large-moment solution, for $I = 0.82$ eV, is instead much more robust with respect to the ordering vector and doping, in good agreement with self-consistent LSDA calculations. The AFM solution possesses two important, general features, which are easily understand-

able in terms of the NM band structure. The value of the magnetic moment is sensitive to the ($FeAs_4$) tetrahedral angle, because it is suppressed by increasing *p–d* covalency, which is strong at all energy scales; the magnetic moment is not orbital polarized, which is a consequence of the small crystal field splittings. On the other hand, the part of the non-magnetic band structure which contributes to forming the magnetic moment is different in the small and large-moment regimes.

In fact, the SDW perturbation couples states at $\mathbf{k}$ and $\mathbf{k}+\mathbf{Q}$, with *common d-character*, opening a gap $\leq\Delta$ between up and down spin states; therefore, only states in an energy range Δ around the Fermi energy contribute to the formation of the moment. $\Delta = 180$ meV for $m = 0.3\,\mu_B$, and $\Delta = 1800$ meV for $m = 2.0\,\mu_B$. As a result, for $m = 0.3$, the magnetic moment is mainly determined from the hole states close to the E_F at $\bar{M}$,($\bar{\Gamma}$) having common *xz*(*xy*) character with electron states at $\bar{X}$,($\bar{Y}$), and is strongly connected to nesting. On the other hand, for $m = 2.0\,\mu_B$, $\Delta = 1800$ meV, so that the whole band structure undergoes a major rearrangement, and the effect of Fermi surface nesting is completely washed out. This implies that the AFM instability found by LSDA calculations is not directly connected to Fermi surface nesting, as it is often argued in literature.

In summary, we have derived *ab initio* an accurate TB model for the non-magnetic band structure of the new iron-based superconductor LaOFeAs. We have used it to explain the main features of the non-magnetic band structure, and shown that many descend from the strong covalency between localized Fe *d*- and diffuse As *p* electrons. As a first application, we have studied the itinerant magnetism with a Stoner model, to try to reconcile the observed disagreement between LSDA calculations and experiment in the estimate of magnetic moments. We have shown that in order to reduce the value of the magnetic moment from the LSDA value $m = 2.0\,\mu_B$ to the experimental value $m = 0.3\,\mu_B$, it is sufficient to reduce the the (Stoner) exchange coupling parameter I by $\approx 20\%$, i.e., from $I = 0.82$ eV to $I = 0.59$ eV. We have argued that the small and large-moment regimes have different origin, and that the AFM instability found by LSDA is not connected to Fermi surface nesting.

The empirical observation that the weak (intermediate) coupling regimes of the same mean-field model for magnetism accurately describe the magnetic (bonding) properties of the same compound, signals that electronic correlations play a non-trivial role in the FeBSC, affecting both low and intermediate energy scales.

[1] *Kamihara, Y., T. Watanabe, M. Hirano, H. Hosono.* Journal of the American Chemical Society **130**, 3296–3297 (2008).

[2] *Boeri, L., O.V. Dolgov, A.A. Golubov.* Physical Review Letters **101**, 026403 (2008) and Physica C **469**, 628–634 (2009); *Mazin, I.I., M.D. Johannes, L. Boeri, K. Koepernik and D.J. Singh.* Physical Review B **78**, 085104 (2008).